*Chinese J. Chem. Eng.*, 11 (6) 701 – 708 (2003)

# Preparation and Properties of a New Type of Poly (butylene-terephthalate) with Layered Silicate Nanocomposites*

**KE Yangchuan(柯扬船)**
State Key Laboratory of Heavy Oil Processing, University of Petroleum, Beijing 102249, China

**Abstract** In this paper, poly(butylene-terephthalate)-layered silicate of clay nanocomposites (NPBT) are reported. Their thermal properties, heat distortion temperature (HDT) and crystallization nucleation are investigated. NPBT samples have apparent viscosity over 0.85, HDT of 30℃ to 50℃ higher than that of poly (butylene-terephthalate) (PBT) for clay load from 1.0% to 10.0% (by mass), and higher capability to accommodate clay than other polymers. The nonisothermal crystallization experiments indicate that the better thermal degradation behavior and crystallization rate of NPBT are 50% higher than PBT, and its injection mould processing temperature is lowered from 110℃ to 55℃. NPBT samples are characterized by several techniques. X-ray shows an original clay interlayer distance enlarged from 1.0 nm to 2.5 nm, while both TEM and AFM indicate an average size from 30nm to 100nm of exfoliated clay layers, and 3%(by mass) of particle agglomeration being phase separated from PBT matrix, which are factors on some mechanical properties decrease of NPBT. The disappearance of spherulitic morphology in NPBT resulted from layers nucleation is detected. Improving NPBT properties by treating clay with long chain organic reagent and controlling the way to load it is suggested.
**Keywords** poly(butylene-terephthalate)-layered silicate of clay nanocomposites, crystallization nucleation, thermal properties, phase separation

## 1 INTRODUCTION

Poly(butylene-terephthalate) (PBT) is one of the top five engineering plastics with such good properties as high crystallization rate, high electrical and mechanical properties, which make it possible to be applied to several fields in engineering reinforced plastics, computer and automobiles, and in different machine parts as gears, engine cylinders, shells of mobiles and voltage adjuster, *etc.* Its disadvantages of low heat distortion temperature (HDT), poor thermal properties and sensitive variation to processing conditions have limited its wider application, and the product share of engineering plastics in the world. So, their processing behavior through modifications is of special importance and significance.

Generally, organic PBT polymer forming nanocomposite with inorganic phase is one of the most popular modification methods today. Layered silicate of clay (briefly clay, hereinafter) is a proper choice of inorganic phase. It has layer unit structure of 50 nm×100 nm×1 nm, where 1nm is its interlayer distance. Such layer structure will be further exfoliated and create nanoparticles in intercalation reaction. So far, polymer-clay nanocomposites are mainly prepared through such an intercalation-polymerization process, which is briefly divided into three approaches as below.

(1) Melting intercalation. Polymer pellets and treated clay are directly mixed in the extruder and then are melt extruded together to obtain the nanocomposites with the exfoliation of layers. The polymer matrix for preparing nanocomposites by such methods are polypropylene (PP)[1−3], polyethylene (PE)[1], polyamine 6 (PA6)[4], polystyrene (PS)[5], *etc.*

(2) Polymerization intercalation. In this method, monomer of polymer is mixed with clay first, then the mixture is polymerized under the reaction conditions similar to polymer without clay addition, during which layers are in-situ exfoliated into nanoparticles. Such polymers for intercalation are PS[6], PA6[7−9], polyimides(PI)[10], poly (ethylene-terephthalate)(PET)[11,13,15], PBT[12−14], polyamine 66(PA66)[16], *etc.*

(3) Media Intercalation. The word "media" here refers to solvent, reagent, gas *etc.* By using the media, clay is treated and then becomes suitable to be applied for different purposes. Polymers for nanocomposites in such a method are PI[10], PET[11], poly (ethylene-oxide) (PEO)[17−19], poly(1-lactide) (PLLA) and poly(ε-caprolactone)(PCL)[20].

Out of so many reports as above for polymer-clay nanocomposites, there are few successful cases. So far, only PA6-clay nanocomposites[21−26] and PET-clay nanocomposites[11,15,16] are successful and prac-

Received 2003-04-08, accepted 2003-09-29.
* Supported by China National Petroleum Corporation Innovation Foundation (No. J02060) and Subsidized by Special Funds for Major State Basic Research Projects (No. G1999064800).

tical.

In this paper, preparing poly(butylene-terephthalate)-clay nanocomposites (NPBT) with clay load from 1.0% to 10.0%(by mass) is prepared, and their properties and morphology are investigated. The structure and properties of NPBT are further investigated by microscopy such as TEM and AFM, *etc.* to show the homogeneity of nanoparticle distribution, the nucleation of exfoliated particles, and cross-linking with PBT molecular chains. Several improvements on NPBT properties are also suggested.

## 2 EXPERIMENT AND CHARACTERIZATION

### 2.1 Materials

The raw clay was obtained from Jianpin, Liaoning Province, China. Its original data were 100 $\mu$m in particle size with cation exchange capacity of 0.7—1.1 mmol·g$^{-1}$ in average, and total $Fe_2O_3$ content less than 0.5%(by mass). This clay was milled to 2—30 $\mu$m in particle size, among which, particles smaller than 17 $\mu$m account for 58%(by volume) by Zata Sizer 2000HS PCS (V14 type), Malvern Co.. This prepared clay was used to produce PBT-clay nanocomposites.

Monomer of 1,4-butylene diol, industrial grade, was from Beijing City Chemical Institute, while dimethyl terephthalate (DMT), industrial grade, from Polyester Plant of Yanshan Company, Beijing, SINOPEC. The catalyst of $Ti(OC_4H_9)_4$ is analytical grade, while all other related solvents and reagents were chemical grade from Dongfang Chemical Factory, Beijing (which now owned by SINOPEC).

### 2.2 Pretreatment of clay for polymerization

Clay was treated with organic reagents as suggested by the literature reports[14,16–18] with only small modification. Taking laurilamine as an example, the treating process is as follows: at first, 20.0 g of montmorillonite clay with cation exchange capacity of 0.9 mmol·g$^{-1}$ was put into 400 g of pure water for wetting 60 min, then the suspension was rapidly stirred. The reaction product of 2.40 g laurilamine with 1.51 g 85% (by mass) phosphorus acid dissolved in 50.0 g pure water was added in. And last, the final intercalated clay was prepared after reaction for 6—12 h. For different treatment reagents, the procedure was kept the same as the above. In such a way, treated clay is prepared suitable for the following polymerization.

### 2.3 Preparation of PBT-clay nanocomposites

In a 50 L autoclave equipped with an anchor stirrer of $\phi$270 mm, and a magnetic driving and stabilizing system (which will ensure the high vacuum level), 2426.25 g of DMT and 1573.15 g of 1,4-butylene diol (BD) were put into the autoclave (molar ratio of BD/DMT was 1.4—2.2), to which the treated clay suspension was added meanwhile the mixer temperature began to rise. Then, TBTT [tetrabytyl titanate, $Ti(OC_4H_9)_4$] was added in total quantity from $4 \times 10^{-5}$ g to $7 \times 10^{-5}$ g Ti per gram DMT to the above mixed solution together with the additive catalyst of $SnO(OH)(n\text{-}C_4H_9O)$ made from Chemical Institute of Beijing City, Beijing. The catalysts were added in two steps. In the first step, half of catalyst was added. After temperature rose up to 90℃, the mixture dewatering starts until water content lower than 1.0% or so. And then, transesterification reaction began for 2—4 h from 140℃ to 220℃. At the end of this stage, another additive of 0.05 g of hexal diamine [$H_2N\text{-}(CH_2)_6\text{-}NH_2$] was added to the above ester product to adjust polymer's molecular weight, and the other half of catalyst was added immediately. Polymerization reaction lasted for 1—3 h under 240℃ to 270℃ and vacuum below 80 Pa. The final product was obtained by dumping the reaction mixture into cool water and cutting it into pellets.

### 2.4 Preparation of film samples

NPBT pellet samples were vacuum-dried at 100℃ to 120℃ for 4 h. Then, they go through a melt-quench process under the heating temperature of 10℃ above their melting points with pressure 50MPa or so under a compressor of oil hydraulic pressure. After melting for 5 min, they were withdrawn from the compressor rapidly, and put into the mixture of water and ice immediately to prepare an amorphous films. When a 1 mm mould was adopted by such a process of melt-quench process, a film thickness of 1mm was prepared for further measurement.

### 2.5 Characterization

#### 2.5.1 *Viscosity*

NPBT samples were dissolved in mixed solvents of 50/50(by mass) of 1,1,2,2-tetracholoro ethane ($n_0^{25}$ = 1.5250) and phenol, and were then measured with Ullman viscometer with a concentration of 0.001 g·ml$^{-1}$ at temperature of (25±0.1)℃.

$$[\eta] = \left(1 + \frac{\eta_{sp}}{0.7c}\right)^{1/2} - 1 \qquad (1)$$

where, $\eta$, intrinic viscosity; $\eta_{sp} = (t - t_0)/t_0$, $t$, $t_0$, time for sample solution flow and pure solvent flow in the viscometry; $c$, concentration of solution (from $1 \times 10^{-3}$ g·ml$^{-1}$ to $10 \times 10^{-3}$ g·ml$^{-1}$ ).

#### 2.5.2 *Mechanical test*

The test included measurements of flexural(bending) and breaking strength according to ASTM 790, and Notched izod impact strength according to ASTM D256. These details were found in the Ref. [13].

**2.5.3** *TEM morphology*

PBT and NPBT samples were embedded in the epoxy. Then, the ultrathin microtome section films (50—100 nm) were cut under microtome diamond knife. The films were moved to the copper grids of TEM, and were dyed in the vapor of $OsO_4$ in the cabinet. TEM observation operates under voltage 200kV on Hitachi S-800H.

**2.5.4** *AFM morphology*

The samples for AFM measurement were obtained by melt-quench process as described above. Film with smooth surface and size in 10 × 10 mm was prepared. AFM was measured on Digital Instrument (Japan Co.)-Nano-Ⅲ. The constant-height mode was adopted to observe the molecule and atom in them. The signal picture on $z$-direction cantilever was recorded. The enlarging effect of particle size was corrected by an factor of 1.1 to 2.0.

**2.5.5** *DSC and TGA*

DSC patterns were obtained by scanning the samples with rate of 10℃ from 30℃ to 270℃ on PE DSC-7 with error of ±1℃ for melt point, while ±5% for $\Delta H$. The nonisothermal crystallization experiment was carried out, at first, the pellets with mass of 2 mg to 6 mg were put into an aluminium crucible, then scanned from 30℃ to 300℃, stayed at 300℃ for 3 min and cooled from 300℃ to 30℃ under different rate (from 5 to 40℃·min). The samples were protected by $N_2$ with flow rate 40 ml·s$^{-1}$. The step-by-step scanning process was designed, and results were corrected by standard matter of tin after each sample. TGA experiment was run on PE TGA-7 with scanning rate of 10℃·min$^{-1}$ from 50℃ to 1000℃ with sample mass between 8 mg to 12 mg.

**2.5.6** *Heat distortion temperature (HDT)*

Samples for HDT measurements are sized of 120 mm×10 mm×12 mm according to GB-1634-79, where polydialkylsiloxane is used as media referred to ASTM D648. The exerted mass is 4.6 kg (equivalent to pressure of 1.84 MPa). The final results are the average of two samples.

## 3 RESULTS AND DISCUSSION

### 3.1 Nanocomposite physical and mechanical properties

NPBT nanocomposite samples with clay load from 1.0% to 10.0%(by mass) were obtained by intercalation-polymerization techniques[11−16] with their results listed in Table 1. In Table 1, $d_{001}$ is clay layer interdistance calculated from Bragg equation[13−15] as $2d_{001}\sin\theta = \lambda$ according to diffraction peak of (001). In NPBT, clay layer interdistance is expanded from 1.12 nm to 2.5 nm over (similar result refers to NPET[13]). This obvious increase is resulted from the intercalation of polymer chains into the interlayer space of clay. This interdistance enlargement directly affects particle size of the final nanocomposites. In Table 1, all viscosity of NPBT is over 0.85 though clay load reaches up to 10% (by mass). The results strongly show that PBT can accommodate more clay content than those of other polymers as PET[15,16], and is not sensitive to clay load when polymerizing, which is advantage as to PBT modifications.

**Table 1 Properties and structure of NPBT for clay treated with laurilamine**

| Clay loading % | $d_{001}$ nm | $\eta$ dl·g$^{-1}$ | $D$ nm | $\sigma_b$ MPa | $E_b$ MPa | Izod J·m$^{-1}$ |
|---|---|---|---|---|---|---|
| 0 (PBT) | - | 0.90 | - | 105 | 1700 | 44.3 |
| 1.0 | - | 0.92 | 20—100 | 110.9 | 2650 | 45.1 |
| 2.0 | - | 0.86 | 30—100 | 106.8 | 2900 | 41.2 |
| 5.0 | 2.5 | 0.87 | 30—100 | 104 | 3700 | 37.4 |
| 10.0 | 2.6 | 0.85 | no results | 95.2 | brittle | brittle |
| 100(clay) | 1.12 | - | - | - | - | - |

Notes: $\eta$, viscosity, dl·g$^{-1}$ (=10$^3$ ml·g$^{-1}$); $D$, particle diameter by TEM statistics; izod, notched izod impact strength; $\sigma_b$ and $E_b$,bending strength and modulus.

The mechanical properties of NPBT, such as the modulus are enhanced greatly. The modulus of NPBT is above 2 times that of PBT when clay loads up to 5%(by mass). Its bending strength is slightly higher than PBT when loading of clay is within 2%(by mass). Sample notched IZOD test shows that IZOD almost unchanged within the loading of 2%(by mass). NPBT tensile strength with clay of 5%(by mass) is enhanced and its tensile modulus increases obviously from 790 MPa of PBT to 1300 MPa of NPBT. So, to balance the properties, loading 2%—5%(by mass) of clay to PBT seems advantageous.

### 3.2 Thermal properties

**3.2.1** *Heat Distortion Temperature*

HDT is a key index for its resistance to heat conditions. Its plot of HDT-clay load is shown in Fig. 1, showing that addition of tiny clay enhances HDT of PBT as obvious nanoparticle effect and /or strong interaction between dispersed clay layers in PBT matrix. The selected reagents have also a great effect on HDT. These organic or intercalation reagents are listed in Table 2, where NPBT has its HDT enhanced from 30℃ to 50℃ over PBT within 5%(by mass). Such increase level of HDT is even greater than that of NPET[15,16], giving thus a new type of PBT material for further modification.

Besides, the relationship of HDT with intercalation reagents shows that,for kinds of reagents selected for treating clay in Table 2, not only the chain length but also the chain polarity of treating reagents, their match with polymer chains, and the loading treated

clay, all have contribution to the HDT of NPBT samples. These results are different from the previous reports on other polymer-clay nanocomposites[21–26], and show that the reagents selected have obvious effect on clay layer dispersion, and its interaction with PBT molecular chains.

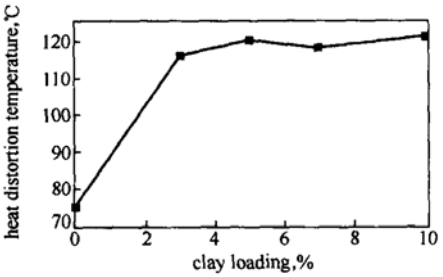


**Figure 1 The plot of HDT-clay load (by mass) for NPBT, where clay is treated by laurilamine as an intercalent**
(see section 2 for the preparation)
—■— HDT-clay NPBT

**Table 2 HDT of NPBT with different clay load and intercalation reagent**

| Interclation reagents | Clay content (by mass),% | Heat distortion temperature*, ℃ |
|---|---|---|
| No | 0.0 | 75 |
| $HOOC(CH_2)_5NH_2$ | 3.0 | 112 |
| $HOOC(CH_2)_5NH_2$ | 5.0 | 120 |
| $CH_3(CH_2)_{11}NH_2$ | 3.0 | 116 |
| $CH_3(CH_2)_{11}NH_2$ | 5.0 | 120 |
| $CH_3(CH_2)_{15}NH_2$ | 3.0 | 118 |

* Measured under the load of 1.84 MPa.

### 3.2.2 *Non-isothermal crystallization behavior*

The crystallization for both PBT and NPBT is investigated by DSC at different scanning rate. Their non-isothermal crystallization is described by Avrami equation as follows

$$\ln\{-\ln[1-X(t)]\} = \ln k + n\ln t \qquad (2)$$

where, $X(t)$ is crystallization degree at time of $t$, $k$ is crystallization dynamic parameter, and $n$ is Avrami number which reflects the growth way of crystallites. The reciprocal value of time $t$ at $X(t) = 50\%$ is applied to express crystallization rate, and Eq. (2)is transformed into Eq. (3)

$$t_{1/2} = \left(\frac{\ln 2}{k}\right)^{\frac{1}{n}} \quad \text{or} \quad \frac{1}{t_{1/2}} = \left(\frac{\ln 2}{k}\right)^{-\frac{1}{n}} \qquad (3)$$

Using Avrami equation to calculate the non-isothermal crystallization data in DSC scanning patterns, their plots of $\ln\{-\ln[1-X(t)]\}$ *vs.* $\ln t$ is obtained and shown in Figs. 2(a) and (b).

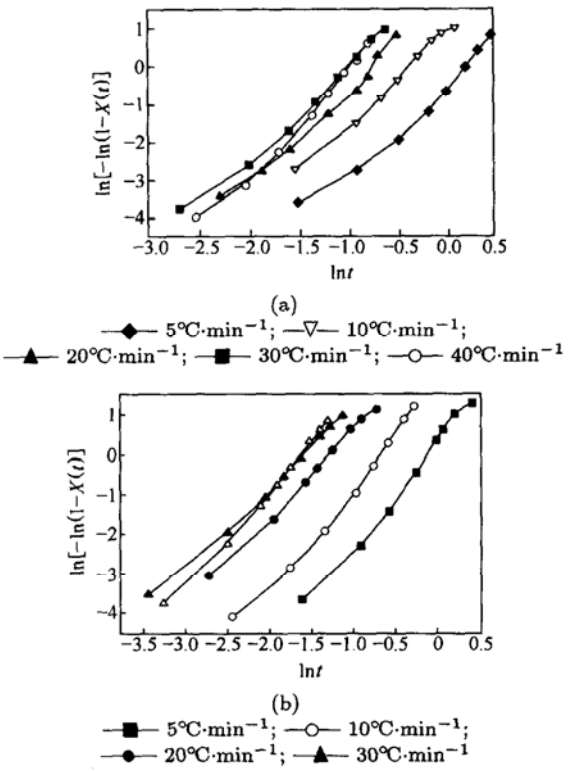


**Figure 2 Nonisothermal crystallization behavior from DSC heating by Avrami equation, for PBT (a) and NPBT (b) with clay load of 5%(by mass)**
(its preparation similar to that in Fig. 1)

From Fig. 2, it is seen that under nonisothermal crystallization at different scanning rate, NPBT (b) and PBT (a) show slight by different crystallization processes at higher scanning rate from 20℃·min$^{-1}$ to 40℃·min$^{-1}$. For NPBT, crystallization curves of 30℃·min$^{-1}$ and 40℃·min$^{-1}$ intersect, while for PBT curves from 20℃·min$^{-1}$ to 40℃·min$^{-1}$ intersect, but at low scanning rate, NPBT and PBT have similar crystallization behavior. These suggest that clay load has a critical point.

Based on the intercept and slope from curves in Fig. 2, parameters of $k$ and $n$ are calculated and listed in Table 3 according to (3). And, the plot of crystallization rate $(1/t_{1/2})$-scanning rate under non-isothermal crystallization is shown in Fig. 3.

**Table 3 Dynamics parameters for PBT and NPBT under non-isothermal crystallization**

| Sample | | Scanning rate, ℃·min$^{-1}$ | | | | |
|---|---|---|---|---|---|---|
| | | 5 | 10 | 20 | 30 | 40 |
| NPBT0 | $t_{1/2}$ | 1.063 | 0.592 | 0.407 | 0.317 | 0.334 |
| | $n$ | 2.24 | 2.38 | 2.34 | 2.36 | 2.69 |
| NPBT5 | $t_{1/2}$ | 0.832 | 0.478 | 0.262 | 0.191 | 0.187 |
| | $n$ | 2.39 | 2.31 | 2.05 | 1.86 | 2.20 |

Notes: NPBT0 stands for pure PBT; NPBT5 stands for PBT loaded with 5%(by mass) of clay, where clay is treated by laurilamine through observing the preparation method in section 2.3.

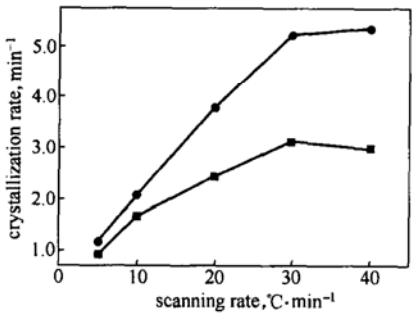


**Figure 3 The plot of crystallization rate-scanning rate under non-isothermal crystallization for both PBT and NPBT with clay load of 5%(by mass)**
(its preparation similar to that in Fig. 2)
—●— NPBT; —■— PBT

It is clearly seen in Fig. 3 that crystallization rate ($1/t_{1/2}$) for NPBT increases rapidly with DSC scanning rate, and especially,the increase scope becomes larger and larger as scanning rate strongly showing much higher crystallization behavior of NPBT than that of PBT. The average increase of NPBT crystallization rate is about 50% higher at all nonisothermal crystallization case than that of PBT within 5% loading of clay. Introducing nanoparticles into its matrix to act as new nucleation centers has direct effect on crystallization rate. But, comparison of all values of $n$ index for both PBT and NPBT in Table 3, the crystallites grow in a similar manner, implying that these nanoparticles are of similar size.

### 3.2.3 *Degree of crystallization*

The crystallization degree is another parameter describing NPBT crystallization behavior. It is expressed as $\Delta H/\Delta H_f^\circ$, where $\Delta H$ is heat of fusion changing as scanning rate and crystallization time, while $\Delta H_f^\circ$ is a heat of fusion at equilibrium state ($\Delta H_f^\circ$ is a fixed value for PBT). The plot of heat of fusion-DSC scanning (non-isothermal crystallization) is shown in Fig. 4

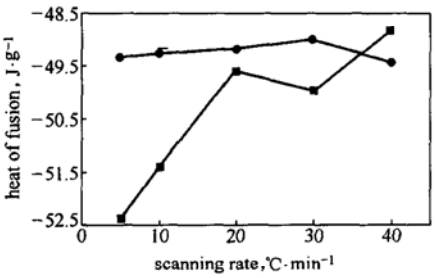


**Figure 4 The plot of heat of fusion ($\Delta H$)-scanning rate under non-isothermal crystallization for PBT and NPBT with clay load of 5%(by mass)**
(its preparation similar to that in Fig. 2)
—●— PBT ; —■— NPBT

In Fig. 4, there is a great difference in crystallization degree (heat of fusion) between PBT and NPBT. $\Delta H$ for NPBT increases much more rapidly than that of PBT with the scanning rate. $\Delta H$ of PBT keeps nearly unchanged under non-isothermal crystallization scanning, suggesting that PBT is slow to respond to scanning rate.

### 3.2.4 *Thermal degradation and melting*

The thermal degradation behavior is shown in Fig. 5 [NPBT5 stands for samples with clay load of 5%(by mass)], showing that they both decompose almost at the same temperature at initial stage. The degradation temperature of other NPBT samples is shown in Table 4 and NPBT is only marginally better than PBT in thermal decomposition.

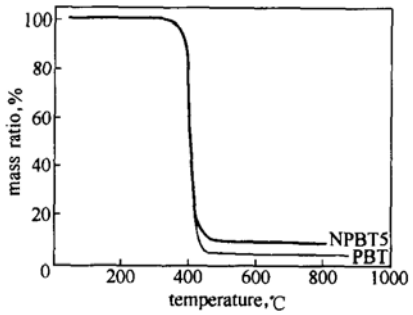


**Figure 5 TGA Scanning Patterns of PBT(a) and NPBT(b) with 5%(by mass) of clay load**

**Table 4 Thermal properties and process properties with laurilamine**

| Sample | Clay loading, % | $T_d$, ℃ | $T_m$, ℃ |
|---|---|---|---|
| NPBT0 | 0.0 | 389 | 231 |
| NPBT5 | 5.0 | 391 | 230 |
| NPBT7 | 7.0 | 401 | 221 |
| NPBT10 | 10.0 | 395 | 223 |

Note: $T_m$, melting point; $T_d$, thermal degradation temperature; the sample nomenclature is the same as in Table 3.

## 3.3 The processing properties

The above superior thermal behavior of NPBT to PBT is of much significance to PBT processing property, specially its injection processing property (I.T.) shown in Table 5.

**Table 5 The processing properties of NPBT with clay load**

| Sample | Clay loading, % | I.T.*, ℃ | Product surface |
|---|---|---|---|
| NPBT0 | 0.0 | 110 | Bright and smooth |
| NPBT5 | 5.0 | 55 | Bright and smooth |
| NPBT7 | 7.0 | 57 | Bright and smooth |
| NPBT10 | 10.0 | 58—60 | Little bright |

* I.T. injection mould temperature for a moulded sample capable of being separated from the mould; the sample nomenclature is the same as in Table 3.

It is well-known that in injection technology, low mould temperature is the key to improve the production efficiency or quantity. In Table 5, I.T. of PBT is much higher than that of NPBT, meaning higher production efficiency. In fact, this has led to 3 times of

production efficiency enhancement comparing to PBT itself. Such a better process is resulted from the formation of the mentioned tiny spherulitic crystallites in NPBT, which lowers its melting point, and forms many nucleation centers to accelerate PBT crystallization.

### 3.4 Structure and properties

#### 3.4.1 *TEM Morphology*

The nucleation effect of clay is proved by TEM morphology, shown in Fig. 6. In Fig. 6(a), spherulite and lamellae in PBT matrix are clear, but their growth is hindered and disappears by introducing clay particles in Fig. 6(b). Dispersed particles have inhibited the growth of spherulites (many attempts have been tried to find spherulites in NPBT, but failed. And even their spoke did not show at all). Here, it is hard to distinguish the nanoparticle from non-nanoparticle in their contributions to NPBT morphology because clay itself exists in crystal form. In PBT, there exist at least two kinds of spherulites, normal and abnormal ones. It seems that only one kind of spherulites is shown by TEM. The reason for the increase of NPBT crystallization rate is thought to be resulted from these fine crystallites, which form more nucleation centers with similar size, grow more rapidly than PBT crystallites itself. When polar reagent ethanolamine is used [Fig. 6(b)] to treat clay, its layers are exfoliated satisfactorily though there some stacked layers still seen. TEM morphology of clay treated by non-polar reagent laurilamine for NPBT shows little layer agglomerations (graph not included). That is, a long chain (*e.g.*, laurilamine) or polarization chain (*e.g.*, short chain of ethanolamine) have slight different effects on properties of NPBT.

When clay load surpasses 5.0%(by mass), layer agglomeration increase obviously from 200 nm to 1000 nm. By TEM statistical data[15], 3%(by mass) or so of agglomeration with micron-size of layers is obtained, which are in phase separation from polymer matrix [Fig. 6(b)]. These agglomerations have effects on PBT properties. And, that clay load to PBT can reach up to 10%(by mass) in polymerization intercalation is an advantage and of much significance to PBT, indicating that NPBT is not much sensitive to clay loading and can accomodate more clay than other polymers as PET, PS, *etc.* It is expected that NPBT with variable clay load will meet the engineering requirements and provide a new raw material for further modification, *e.g.*, NPBT in high clay load with unexfoliated particles will be applied as an engineering plastics.

#### 3.4.2 *AFM*

To investigate nanoparticle distribution, their stability and phase separation in NPBT, they are subjected to melt-quench process from 250℃ to the ice water. Their AFM morphology is shown in Fig. 7, where the friction-force experiment mode is taken for measurement.


(a)


(b)

**Figure 6 The TEM morphology for PBT spherulitic (a), for NPBT with clay loading of 2%(by mass) by polarized reagent(b)**

In Fig. 7(a), some area with bright stacked particles in NPBT is specially chosen to show the agglomerations with clay load of 5%(by mass). When discounting the expanding effect from AFM needle, few stacked particles are detected to be greater than 100nm in size, which is consistent with these of TEM in Figs. 7(b) and (c). These bright particles are 1.0nm or so higher than these dark part (polymer matrix). The particles greater than 100 nm in Fig. 7(a) are phase separated from the matrix, compared with morphology in Fig. 7(b). For this same NPBT sample and the axis scale from 0 nm to 20 nm, its finer structure is seen in Fig. 7(b), where the probable long range ordered structure is called secondary nanostructure[4,9,15] which depends on the dispersed layers and their morphology. In Fig. 7(b), the bright domains are higher than that of the dark, standing for particle phase separation from PBT matrix in $Z$-dimension. When the morphology in Fig. 7(b) projected to a plane shown in Fig. 7(c), some regular patterns are seen there. And, there exists a long range of order of bright domains in the direction of 45° to the $Y$-axis. These regular patterns of quenched NPBT are mixed up from crystallites

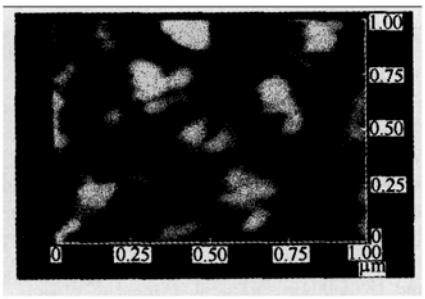


(a) Stacked particle morphology in some area of NPBT with clay load of 5%(by mass)

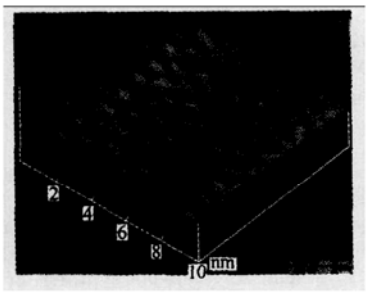


(b) An island morphology of particle agglomeration and a phase separation from the matrix

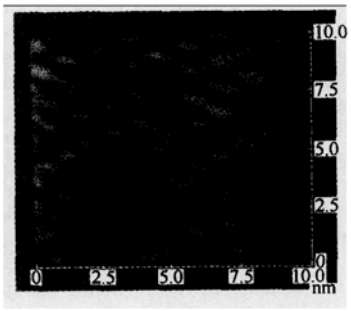


(c) A projection of secondary structure of the island morphology

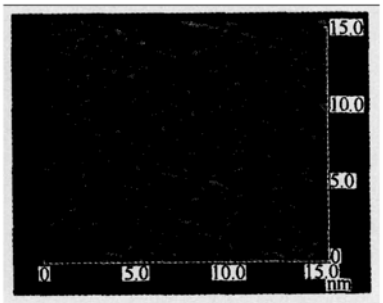


(d) Secondary morphology for clay load of 3%(by mass) showing order area

**Figure 7 AFM morphology of quenched NPBT films**

of polymer PBT and dispersed layers or clay crystal layer, and reflect a molecular order resulted through the absorption of polymer chains to the surface of clay, whose morphology become clear when more refined structure of clay is detected in Fig. 7(d), where the dispersed layers are very dense and homogeneous in NPBT.

The bigger crystals of clay tend to be excluded by both crystal and amorphous domains of PBT, implying that in polyester based nanocomposites with clay, the particle agglomerations are unavoidable. Their phase separation from PBT is a factor to its reduction of mechanical properties. In other words, some exfoliated layers are unstable and will assemble again to stack together.

## 4 CONCLUSIONS

By loading clay to PBT matrix from 1% to 10%(by mass), NPBT samples are prepared. Compared to PBT, HDT of NPBT is increased by 30℃ to 50℃, modulus is enhanced greatly, and good processing property or low injection temperature of moulding process and 50% higher crystallization rate than that of PBT are obtained. PBT has more capacity to accommodate clay than the other polymers. Investigations of NPBT show that nanoparticles range from 30 nm to 100 nm with 3% agglomeration of layers in phase separation from PBT matrix. The layer agglomerations and phase separation in NPBT make its mechanical properties decreased.

## ACKNOWLEDGMENTS

*Part of this work is supported by BASF Co. under Sino-Germany cooperation project. The support of this work by the state key lab of heavy oil processing is highly appreciated.*

## NOMENCLATURE

| | |
|---|---|
| $c$ | concentration of a solution, g·ml$^{-1}$ |
| $d$ | diameter of a particle, nm |
| $d_{001}$ | interdistance of diffraction face at crystalline face (001), nm |
| $E_b$ | bending modulus, MPa |
| $\Delta H$ | Heat of fusion, J·g$^{-1}$ |
| $\Delta H_f^\circ$ | a heat of fusion at equilibrium state, J·g$^{-1}$ |
| $k$ | crystallization dynamic parameter |
| $n$ | Avrami number |
| $T_d$ | thermal degration temperature, ℃ |
| $T_m$ | melting point, ℃ |
| $t$ | time, s |
| $t_{1/2}$ | The reciprocal value of time $t$ at $X(t) = 50\%$, s |
| $X(t)$ | crystallization degree at time of $t$ |
| $\eta$ | viscosity |
| $\sigma_b$ | bending strength, MPa |

## REFERENCES

1 Hudson, S.D., "Polyolefin nanocomposites", US5910523 (1999).
2 Kawasumi, M., Hasegawa, N., Kato, M., Usuki, A., Okada, A., "Preparation and mechanical properties of PP-Clay hybrids", *Macromolecules*, **30**, 6333 (1997).
3 Zhang, Q., Fu, Q., Jiang, L.X., Lei, Y., "Preparation and properties of polypropylene-clay nanocomposites", *Polymer International.*, **49** (12), 1561 (2000).

4 Lincoln, D.M., Vaia, R.A., Wang, Z.G., Hsiao, B.S., "Secondary structure and elevated temperature of crystalline morphology of nylon-6/layered silicate nanocomposites", *Polymer*, **42**, 1621 (2001).
5 Lim, Y.T., Park, O.O., "Rheological evidence for the microstructure of intercalated polymer/layered silicate nanocomposite", *Macromol. Rapid Commun*, **21**, 231 (2000).
6 Hoffman, B., Dietich, C., Thomann, R., Fredrich, C., Mulhaupt, R., "Morphology and rheology of polystyrene nanocomposites based opon organoclay", *Macromol. Rapid Commun*, **21**, 57 (2000).
7 Qi, Z., Li, Q., Zhou, Y., "A kind of Polyamide-clay nanocomposites and its preparation",CN139643 A (1996). (in Chinese)
8 Vaia, R.A., Ishii, H., Giannelis, E.P., "Synthesis and properties of two-dimensional nanostucture by direct intercalation of polymer melts in layered silicates", *Chem. Mater.*, **5**, 1694 (1993).
9 Vaia, R.A., Vasudevan, S., Krawiec, W., Scanlon, L.G., Giannelis, E.P., "Polymer-layered silicate nanocomposites", *Adv. Mater.*, **8** (1), 29 (1996).
10 Zhu, Z.K., Yang, Y., Ying, J., Wang, X.Y., Ke, Y.C., Qi, Z.N., "Preparation and properties of organo-soluble MMTs/PI hybrid materials", *J. Appl. Polym. Sci.*, **73**, 2063 (1999).
11 Qi, Z.N., Ke, Y.C., Zhou, Y.Z., "A kind of poly(ethylene-terephthalate)-clay nanocomposites and their preparations", Chin.Pat Appl., 971040559. (in Chinese)
12 Qi, Z.N., Ke, Y.C., Zhou, Y.Z., "A kind of poly(butylene-terephthalate)-clay nanocomposites and their preparations", Chin. Pat. Appl., 971041964.
13 Ke, Y.C., Qi, Z.N., Long, C.F., "Crystallization, properties, and crystal and nanoscale morphology of PET-Clay nanocomposites", *J. Appl. Polym. Sci.*, **71**, 1139 (1999).
14 Ke, Y.C., Long, C.F., Internat. Symp. on Polym. Physi., Guilin city, 158 (1997).
15 Ke, Y.C., Yang, Z.B., Zhu, C.F., "Investigation of properties nanostructure, and distribution in controlled polyester polymerization with layered silicate", *J. Appl. Polym. Sci.*, **85** (13), 2677—2691 (2002).
16 Ke, Y.C., "A kind of nanoparticle precursor and its preparation method", CN 02157993.8 (2003).
17 Choi, H.J., Kim, S.G., Hyun, Y.H., Jhon, M.S., "Preparation and rheological characteristics of solvent-cast poly(ethylene-oxide)/montmorillonite nanocomposites", *Macromol. Rapid Commun.*, **22**, 320 (2001).
18 Lu, J.K., Ke, Y.C., Yi, X.S., Qi, Z.N., "Study on intercalation and exfoliation behavior of organoclays in epoxy resin", *J. Polym. Sci., Part B: Polym. Phys.*, **39**, 115 (2001).
19 Ke, Yu.C., Lu, J.K., Yi, X.S., Zhao, J., Qi, Z.N., "The effects of promoter and curing process on exfoliation behavior of epoxy/clay nanocomposites", *J. Appl. Polym. Sci.*, **78**, 808 (2000).
20 Ogawa, N., Jimenez, G., Kawai, H., Ogihara, T., "Structure and thermal/mechanical properties of poly(l-lactide)-clay blend", *J. Polym. Sci. Part B: Polym. Phys.*, **35**, 389 (1997).
21 Kojima, Y., Okada, A., "Fine structure of nylon-6/clay hybrid", *J. Appl. Polym. Sci.: Part B: Polymer Physics*, **32** 625 (1994).
22 Wu, T.M., Liao, C.S., "Polymorphism of nylon-6/clay nanocomposites", Macromol. Chem. Phys., **201**, 2820 (2000).
23 Kojima, Y., Usuki, A., Kawasumi, M., Okada, A., Fukushima, Y., Kurauchi, T., Kamigato, O., "Dispersed structure change of smectic clay/poly(methylmethacrylate) nanocomposites by copolymerization with polar comonomers", *J. Mater. Res.*, **8**, 1185 (1993).
24 Kojima, Y., Usuki, A., "One-pot synthesis of nylon-6/clay hybrid", *J. Polym. Sci.: Part A: Polym. Chem.*, **31**, 1755 (1993).
25 Usuki, A., Mizutani, T., Fukushima, Y., Fujimoto, M., Kojima, Y., Kurauchi, T., Kamigaito, O., "Composite material containing a layered silicate", US4889885 (1989).
26 Hutton, Jr., Alexander, E., Burke, R.E., Wheeler, Jr., Stenley, P., "Water-resistant, water-flushable paper composites",US 49201714 (1990)
27 Kamens, Ernest R., "Unsaturated polyester resin foams using inorganic ion salts", US04460714 (1984)
28 Brereton, M.G., Dowies, G.R., Fakeways, R., "Hysteresis of the stress-induced crystalline phase transition in poly(butenelene-terephthalate)", *Polymer*, **19** (1), 17 (1978).
29 Hall, I.H., Pass, M.G., "Chain conformation of poly(tetramethylene-terephthalate) and its change with strain", *Polymer*, **17**, 807 (1976).
30 Galgali, G., Ramesh, C., Lele, A., "A rheological study on the kinetics of hybrid formation in polypropylene nanocomposites", *Macromolecules*, **34**, 852 (2001).